



The modelling of nonlinear distance sensor using piecewise newton polynomial with vertex algorithm

The case study of sensor performance improvement on the distance measuring sensor unit sharp GP2Y0A02YK0F

Gutama Indra Gandha

Universitas Dian Nuswantoro

01 Nakula Street, No. 5 -11, B Building, Semarang Central Java, Indonesia

Corresponding email: gutama.indra@dsn.dinus.ac.id

Received 16 June 2021, Revised 22 July 2021, Accepted 18 August 2021

Abstract — The Sharp GP2Y0A02YK0F is categorized as a nonlinear sensor for distance measurement. This sensor is also categorized as a low-cost sensor. The higher resolution, cheap, high accuracy, and ease to install are the advantages. However, the accuracy level of this sensor depends on the type of the measured object materials, requires an additional device unit, and further processing is required since the output is nonlinear. The distance determination is not easy for this type of sensor since the characteristic of this sensor fulfills the non-injective function. The modelling process is one of the methods to convert the sensor's output voltage to a distance unit. The advantages of polynomial modeling are simple form model, moderate inflexibilities of shape, well known and understood properties, and easy to use for computational matters. The obstacle of polynomial-based modeling is the presence of Runge's phenomenon. The minimization of Runge's phenomenon can be done by decreasing the model order. The piecewise Newton polynomials with vertex determination method has succeeded in generating a nonlinear model and minimizing the occurrence of Runge's phenomenon. The low level of MSE by 0.001 and error percentage of 2.38% has been obtained for the generated model. The low MSE level leads to the high accuracy level of the generated model.

Keywords – Newton polynomials, nonlinear sensor, vertex, infrared sensor

Copyright © 2021 JURNAL INFOTEL

All rights reserved.

I. INTRODUCTION

The Sharp GP2Y0A02YK0F is categorized as a nonlinear sensor for distance measurement. This sensor consists of three main parts, namely PSD (Positive Sensitive Detector), signal conditioning unit, and IRED (Infrared Emitting Diode). The infrared emission has been used to measure the distance. An LED infrared drive unit emits the infrared to perform the objective measurement. The PSD captures the infrared signal that is reflected by the object. The signal processing unit receives the output signal that PSD generates. The result of the signal processing unit is treated as an output signal [1]. This type of sensor has been implemented in many fields, including an autonomous robots, industrial, smart applications, and aerial navigation. This sensor is also categorized as a low-cost sensor [2][3]. The higher resolution in measurement result is the advantage of the infrared-based distance

sensor. The other advantages are cheap, high accuracy, and ease to install. However, this sensor also has a weakness. The accuracy level of this sensor depends on the type of the measured object materials, requires an ADC (Analog to Digital Converter) unit, and further processing is required since the output is nonlinear [4].

Distance determination is not easy for this type of sensor. The output determination of this sensor requires external hardware and software. The external hardware includes the addition of an ADC (Analog to Digital Converter) device. The external software requirement focuses on the modeling process since the characteristic of the output sensor is nonlinear. The modelling process is one of the methods to convert the sensor's output voltage to a distance unit[5]. Polynomial modeling has been used in many areas. The advantages of polynomial modeling are simple form model, moderate inflexibilities of shape, well known and understood

properties, and easy to use for computational matters. The Newton polynomials are categorized as robust methods for computational purposes [6]. The obstacle of polynomial-based modeling is the presence of Runge's phenomenon. Runge's phenomenon is an oscillation problem when the generated model requires high degree polynomials [7]–[9].

The modeling of nonlinear curves is highly likely to suffer from Runge's phenomenon. The presence of Runge's phenomenon decreases the accuracy level of the generated model [10]. Therefore, it is important to reduce Runge's phenomenon, especially in the modeling process [1]. The robust model with less occurrence of Runge's phenomenon is the aim of this research. The robust model is the most important aspect of the sensor development process. It also directly affects the time and cost in the development stage.

II. RESEARCH METHODS

The nonlinear sensor handling has its challenges, such as calibration, conversion method, and sensor behavior. The nonlinear sensor calibration also has its complexities. The development of the sensor model is a solution when facing nonlinear sensor calibration [5]. In certain cases, the modeling of nonlinear sensors brings more complexity and requires more modeling methods [11]. The solution for nonlinear sensor modeling is the polynomial fitting method. Liqun has developed the virtual instrument for nonlinear sensor calibration. The polynomial fit method has been used in this research. A virtual instrument developed by Liqun has simulated the fiber-optic displacement sensor CSY2000. The virtual instrument produced a low level of error by 0.117 mm. The robust performance of polynomial fit algorithms has been proven by a low level of error [12].

The Deskew algorithm and polynomial fit algorithm have been implemented in this research. Based on the research result, the Deskew filter algorithm resulted in lower performance than the polynomials algorithm. A polynomial algorithm has achieved the improvement of spatial resolution even in the strong noise [13]. The more complexity of the curve requires more degree in the polynomial model. The higher degree of polynomial models leads to the presence of Runge's phenomenon. The appearance of oscillation at the end of the interval is the effect of Runge's phenomenon. The model reduction method is a solution to minimize the oscillation as the effect of Runge's phenomenon occurrence. The model reduction method divides the curve into several parts. By dividing the curve, the lower degree of the polynomial model can be achieved. Igor has proposed the piecewise polynomial method. Igor utilizes piecewise polynomial methods to reduce the model order for nonlinear systems. The nonlinear system has more complexities than the linear system. The piecewise polynomial method can reduce the model order and linearizes the nonlinear model [14]. The lower degree of the model reduced the presence of

Runge's phenomenon [7]–[9]. The model reduction method and polynomial algorithm are commonly used in modeling matter. The collaboration between piecewise polynomials with the vertex determination method and Newton's polynomial algorithm has been proposed in this research. Newton's polynomial algorithm required lower computational cost and produced less error [6]. The vertex determination method determined the dividing point of piecewise polynomials.

Several steps have been performed to address the challenge. First, the data acquisition process has been used to obtain the raw data of the sensor. The next step is modeling without piecewise polynomials with the vertex determination method. When the modeling resulted in the low accuracy model, the modeling featured piecewise polynomials method with vertex determination method would be performed. The last step is model evaluation.

A. The data acquisition of the infrared sensor (GP2Y0A02YK0F)

The working principle of the infrared-based distance sensor is based on infrared reflection. The infrared emitter emits the infrared signal. The receiver captures the reflection of an infrared signal that is emitted by an infrared emitter—this sensor results in analog voltage as the output. The advantage of this sensor is that it is easy to install. This sensor requires an ADC (Analog to Digital Converter) for integration with a microprocessor or microcontroller.



Fig. 1. The GP2Y0A02YK0F sensor unit

The GP2Y0A02YK0F featured three terminals, namely output terminal, voltage supply terminal and the latest is ground terminal. This sensor requires 4.5 – 5.5 VDC as the main supply voltage. Therefore, the minimum output voltage of this sensor is close to 0 Volt and around 2.8 Volt for the maximum output voltage [1]. The pin layout is shown in Fig. 2.

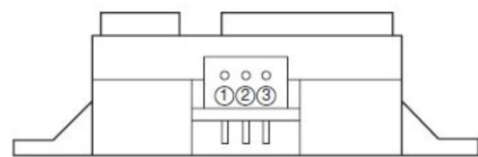


Fig. 2. Pin playout - 1. The output terminal (Vo), 2. Ground (GND), 3. Supply voltage (Vcc) [1].

The technical specification sheet of the sensor shows the sensor has nonlinear characteristics. The

valid measurement distance range of the sensor is between 20 to 150 cm. The ideal nonlinear characteristic of the sensor is shown in Fig.3.

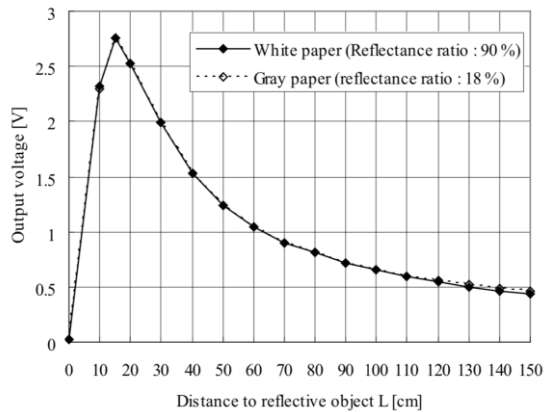


Fig. 3. The ideal characteristic of the GP2Y0A02YK0F sensor unit[1]

The ideal nonlinear characteristic needs to be confirmed using a data acquisition process. The data acquisition process has been performed using a 1 cm interval of the measurement and the distance range by 0-150 cm. The schematic of the data acquisition is shown in Fig.4.

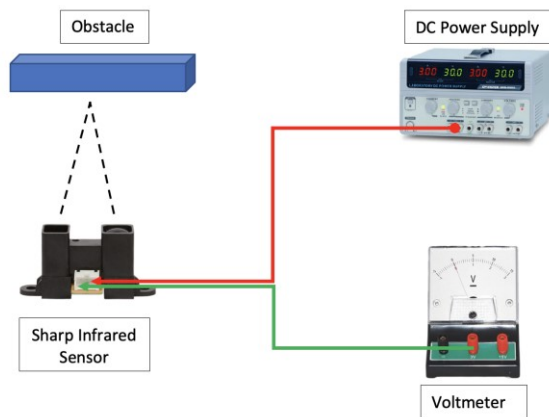


Fig. 4. The schematic of sensor data acquisition.

B. Modeling using Newton polynomial

The Newton polynomial is a polynomial-based modeling method that used high order degree polynomials equation. This method can create models with complex shapes and has several advantages: low error level, low computation cost, and simple form [6]. The data acquisition process results in vector data. The vector has a form of a two-dimensional vector: the vector component, namely distance (cm) and voltage (volt). The Newton polynomial algorithm has been used to obtain the model. Once the model has been obtained, then the accuracy-test would be performed. The analysis regarding the presence of the Runge's phenomenon was also performed in this stage.

C. Modeling using piecewise Newton polynomials with vertex determination algorithm

When the generated model obtained by the previous step results in a low level of accuracy, then the modeling featured piecewise Newton polynomials with vertex determination would be performed. The vertex determination method marks a certain point as a cutting point when the slope is within a certain range of values. This algorithm resulted in 2-dimensional vectors, namely distances and vertex points.

The piecewise Newton algorithm with vertex determination method involving 3 main methods namely vertex determination algorithm, piecewise polynomial algorithm and Newton polynomial algorithm. The flowchart process is shown in Fig.5.

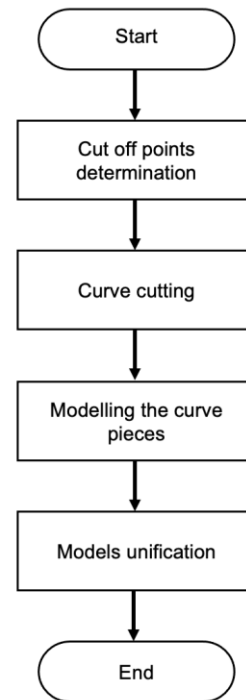


Fig. 5. The flow of modelling process

The accuracy test would be performed when the model has been obtained successfully.

D. Model evaluation

The assessments and evaluation regarding the generated model would be performed in this step. The evaluation compares the performance between the model generated by the Newton polynomial algorithm and piecewise newton polynomial with vertex determination algorithm.

III. RESULTS

The data acquisition process results in a vector that contains two elements: the output voltage measurement and the measured distance. The graphical plot of the vector is shown in Fig.6.

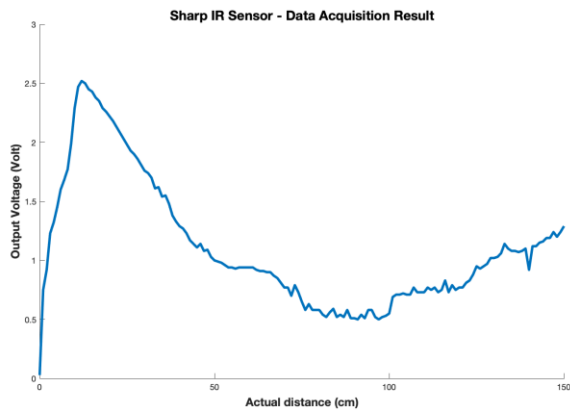


Fig. 6. Data acquisition process result

According to Fig. 6, there is slight difference the ideal characteristic sensor and actual measurement result. The function characteristic of the actual measurement's vector is categorized as a non-injective function. The non-injective function characteristic leads to ambiguity in the input-output relation. The non-injective characteristic is highly possible to produce two different values of output from one input. A particular method is required to address the problem of a non-injective characteristic of this sensor. In the second step, the modeling featured Newton polynomials algorithm has been performed. The result is shown in Fig.7.

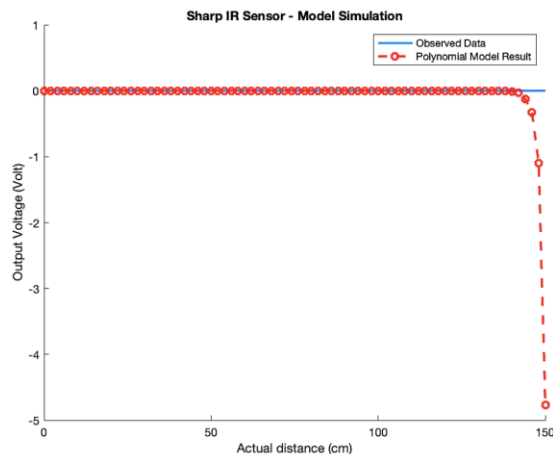


Fig. 7. The presence of Runge's phenomenon

The presence of Runge's phenomenon appears significantly in the generated model, as shown in Fig.7. The high level of Runge's phenomenon leads to the model's instability and decreased accuracy level of the generated model. The reason behind Runge's phenomenon's presence is related to the degree number of the model order. The more degree in the model order leads to the more likely the appearance of Runge's phenomenon.

The Newton polynomials algorithm-generated $n-1$ order degree for the generated model. Where n is the data length of the vector, let's suppose there is a vector with a data length of n , then the resulting polynomial equation must be a polynomial equation with the degree of $n-1$. In this research, the data length of the vector

data is 151. It means the Newton polynomials generated model with 150 of order degree. Such number of the order degree has proven in the leads of Runge's phenomenon significantly. The model degree reduction method is one of the solutions to prevent Runge's phenomenon. The piecewise polynomials method can decrease model order numbers by splitting the model into several parts of models. The vertex determination method has been used to determine the splitting point of the generated model.

The vertex determination finds the correct gradient value between two points along the curve. When the correct gradient value has been found, this method will set the point as a splitting point. The piecewise polynomials used the splitting point obtained by the vertex determination method to split the curve into several parts. The latter, Newton polynomials, generates models from the splitter curves. The usage of the piecewise Newton polynomials with vertex determination method has succeeded in minimizing the occurrence of the Runge's phenomenon. Furthermore, the lower model order has been succeeded to decrease the possibility of Runge's phenomenon appearances. The graphical plot of the generated model is shown in the Fig. 8.

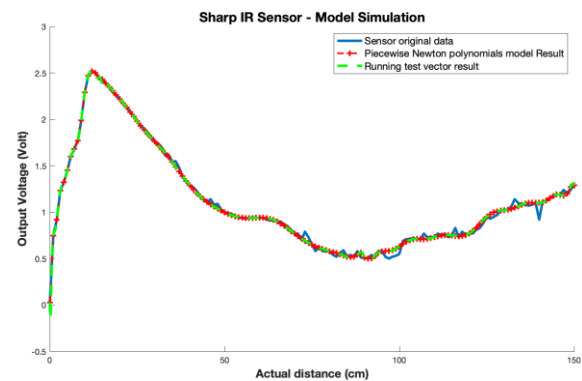


Fig. 8. The result of the model is by using the piecewise newton polynomials method.

IV. DISCUSSION

The modeling process requires four main processes executed sequentially, namely cut-off points determination, curve cutting, the curve pieces modeling, and model unification, as shown in Fig.5. Firstly, the vertex determination algorithm performs the cut-off points determination process. This process results in the cut-off points sets. The cut-off points are then used by a piecewise algorithm in order to cut the curve into pieces. The Newton polynomial algorithm performs the third process. Each curve piece would be modeled automatically by using the Newton polynomials algorithm. This process resulted in several generated models. Finally, the model unification method unifies generated models into one model.

A. Cut off points determination using vertex determination algorithm

The basic operation of the vertex determination algorithm is similar to the derivative method. The derivative formula is shown in Eq. 1

$$\frac{dy}{dx} = \frac{\Delta y}{\Delta x} = \frac{y_2 - y_1}{x_2 - x_1} \quad (1)$$

The vertex determination algorithm indexes the first point until the end of the point of the curve with a certain interval point. The interval point by 5 points has been used in this research. This method checks the angle based on the slope along the curve per 5 points intervals. The conversion formula to perform conversion from the slope to angle is shown in Eq. 2.

$$\theta = \arctan\left(\frac{y_2 - y_1}{x_2 - x_1}\right) \quad (2)$$

$$m \leq \theta \leq n$$

The vertex determination method marks a certain point as the cutting point when θ is higher or equal to m or θ less or equal to n . The symbol of m represents the minimum slope, and the n represent the maximum value of the slope. In this research, the variable of m represented by 0 and n represented by 0.5. This algorithm resulted in marks of cutting points used by a piecewise algorithm to cut the curve.

B. Piecewise algorithm for curve cutting

The main job of the piecewise algorithm is to cut the nonlinear curve into several parts. This algorithm cuts the curve according to the cutting points generated by the vertex determination method. The lower-order degree of polynomials has been successfully generated for each curve piece. The lower-order degree minimizes the presence of Runge’s phenomenon. The equation of piecewise polynomials is shown in Eq.3.

$$y(n) = \begin{cases} H_1[x(n)], 0 < |x(n)| \leq a_1 \\ H_2[x(n)], a_1 < |x(n)| \leq a_2 \\ \dots \\ H_p[x(n)], a_p < |x(n)| \leq a_{p+1} \end{cases} \quad (3)$$

Where $H_i[]$ represents polynomials function for the sensor’s curve, a_i represents the cutting points.

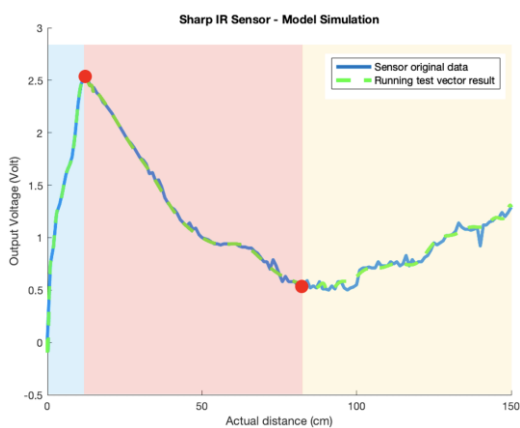


Fig. 9. The curve cutting points of the Sharp infrared sensor curve with vertex points (red dot).

The result shows the curve has been cut into three pieces of curve parts as shown in Fig.9. Each piece of the curves fulfilled the injective function. The injective function leads to the non-existence of ambiguity in the input-output relation of the curves. This curve-cutting process is related to Eq.3. Each color represents a difference curve of H . The curve with the blue area represents $H_1[x(n)]$, $H_2[x(n)]$ represented by a curve with the red area and the curve with yellow area represents $H_3[x(n)]$.

C. Newton’s polynomials modeling

Let assume an input value z_i which represents the measurement distance of the sensor. The function of z_i symbolized as $f(z_i)$. It represents the output voltage of the sensor. The z_i and $f(z_i)$ arranged as a two-dimensional vector. Where i represents the number of the sequence. The z_i and $f(z_i)$ are known values. The D matrix, which has $3 \times n$ size of matrix dimension, has been used to represent the data scheme.

$$D = \begin{bmatrix} 0 & z_0 & f(z_0) \\ 1 & z_1 & f(z_1) \\ n & z_n & f(z_n) \end{bmatrix} \quad (4)$$

Newton’s polynomial computation aims to determine the coefficients and the shape of the model. The coefficient computation involves the matrix of D . Eq. 5 represents the equation that has been used to obtain the coefficient.

$$f[z_k] = f(z) \quad (5)$$

$$f[z_0, z_k] = \frac{f[z_0] - f[z_k]}{z_0 - z_k}$$

$$f[z_0, z_1, \dots, z_i, z_k] =$$

$$\frac{f[z_0, z_1, \dots, z_i] - f[z_0, z_1, \dots, z_{i-1}, z_k]}{z_i - z_k}$$

To simplify the coefficient computation, Newton’s divided difference table has been used in this research. The scheme of Newton’s divided difference table is shown in Table 1.

Table 1. Newton’s divided difference table

$f[z_0]$			
$f[z_1]$	$f[z_0, z_1]$		
$f[z_2]$	$f[z_1, z_2]$	$f[z_0, z_1, z_2]$	
$f[z_i]$	$f[z_{i-1}, z_i]$	$f[z_{i-2}, z_{i-1}, z_{i-0}]$	$f[z_0, z_1, z_2, \dots, z_i]$

Inside the microprocessor, Newton’s divided difference table must be converted into the matrix of T . This matrix contains the whole coefficient for the final model.

$$T = \begin{bmatrix} f[z_0] & 0 & 0 & 0 \\ f[z_1] & f[z_0, z_1] & 0 & 0 \\ f[z_2] & f[z_1, z_2] & f[z_0, z_1, z_2] & 0 \\ f[z_i] & f[z_{i-1}, z_i] & f[z_{i-2}, z_{i-1}, z_{i-0}] & f[z_0, z_1, z_2, \dots, z_i] \end{bmatrix} \quad (5)$$

Based on the matrix of T , the shape of the final model would be formed. The form of the final model equation is shown in Eq. 6. The final model generated by Newton polynomials represented by $p_n([z])$. This algorithm consists of polynomials on n th degree passing through the point of $(z_i, f(z_i))$ where $i = 0, 1, \dots, n$ [36].

$$p_n([z]) = f(z_0) + \pi_1 f[z_0, z_1] + \pi_2 f[z_0, z_1, z_2] + \dots + \pi_n f[z_0, z_1, z_n] \quad (6)$$

Where $\pi_i = (z - z_0)(z - z_1) \dots (z - z_{i-1})$ and $f[z_0, z_1, \dots, z_i]$ is the i th divided difference of f . The shortened formula representation of Newton's polynomial algorithm is shown in Eq.7.

$$p_n(z) = f(z_0) + \sum_{k=0}^{n-1} f[z_0, z_k] \sum_{n=0}^{n-k} (z - z_0) \dots (z - z_{n-1}) \quad (7)$$

D. Model unification

Model unification unites the model pieces into one model. The algorithm of model unification is shown in Eq.8.

$$p(z) = p_1(0 < z \leq a_1) \cup p_2(a_1 < z \leq a_2) \cup \dots \cup p_n(a_{n-1} < z \leq a_n) \quad (8)$$

In this research, the piecewise algorithm divides the curve into three pieces of the curves based on the acquired slopes. Newton's polynomial algorithm performed the modeling for three pieces of the curves. Each curve resulted in one polynomial model. Newton polynomials generate three models. The three models must be combined into one complete model so the model can work properly in the certain input range of z . The model unification algorithm classifies the input quantity based on the limits set in the piecewise algorithm automatically. The limit set lies on the $a_1 \dots a_n$ Parameters. These parameters are equal to the parameters applied to the piecewise algorithm. The final result of the model could be seen in Fig.7. The red dash plot is the final result of the model with an input interval of 5 cm. The closer intervals are also carried out in the testing process. The green dash plot is the final result of the model with an input interval by 0.001 cm. Thus, the model has succeeded to represent the real data of the sensor with satisfying closeness level.

E. The model evaluation

The MSE (Mean Squared Error) and MAPE (Mean Absolute Percentage Error) methods are used to evaluating the model performance. Firstly, the MSE method has been used to evaluate the closeness level of the final model. Therefore, the lower MSE value means a higher level of model accuracy. The MSE equation is shown in Eq.9.

$$MSE = \frac{1}{n} \sum_{i=1}^n (\hat{X}_i - X_i)^2 \quad (9)$$

The data quantity represented by n , the true values represented by \hat{X}_i , and X_i represents the measurement value of i th measurement. By using the MSE method, the MSE level by 0.001 has been obtained. Thus, the low level of MSE has been achieved successfully. The measurement error percentage was also performed in this research. The measurement of error percentage has been performed by The MAPE method. The MAPE equation is shown in Eq.12.

$$MAPE = \frac{100\%}{n} \sum_{i=1}^n \frac{\hat{X}_i - X_i}{\hat{X}_i} \quad (10)$$

The final model of the sensor resulted in an error percentage of 2.38%, or the accuracy level of the final model is 97.62%.

V. CONCLUSION

The Sharp GP2Y0A02YK0F is an infrared-based analog distance sensor. This type of sensor has a higher resolution than an ultrasonic-based distance sensor. Since the characteristic of the sensor fulfilled the nonlinear with non-injective function, the modeling process is one of the methods to convert the output voltage of the sensor to a distance unit. One of the solutions for nonlinear sensor modeling is polynomial fit. The disadvantage of the polynomial fit method is the presence of Runge's phenomenon. The minimization of Runge's phenomenon can be done by decreasing the model order. The piecewise Newton polynomials with vertex determination method have succeeded in generating a nonlinear model and minimizing the occurrence of Runge's phenomenon. The low level of MSE by 0.001 and error percentage of 2.38% has been obtained for the generated model. The low MSE level leads to the high accuracy level of the generated model.

REFERENCES

- [1] D. Measuring and S. Unit, "Gp2Y0a02Yk0F," *Production*, pp. 1–9, 2006.
- [2] P. Malheiros, J. Gonçalves, and P. Costa, "Towards a more Accurate Infrared Distance Sensor Model," *Manuf. Syst. Eng. Unit*, no. Sept, 2010.
- [3] D. M. Sobers, G. Chowdhary, and E. N. Johnson, "Indoor navigation for Unmanned Aerial Vehicles," *AIAA Guid. Navig. Control Conf. Exhib.*, no. August, 2009, doi: 10.2514/6.2009-5658.
- [4] B. Mustapha, A. Zayegh, and R. K. Begg, "Ultrasonic and infrared sensors performance in a wireless obstacle detection system," *Proc. - 1st Int. Conf. Artif. Intell. Model. Simulation, AIMS 2013*, pp. 487–492, 2014, doi: 10.1109/AIMS.2013.89.
- [5] P. J. C. Biselli, R. S. Nóbrega, and F. G. Soriano, "Nonlinear flow sensor calibration with an accurate syringe," *Sensors (Switzerland)*, vol. 18, no. 7, pp. 1–9, 2018, doi: 10.3390/s18072163.
- [6] R. Srivastava and P. Srivastava, "Comparison of Lagrange's and Newton's interpolating polynomials,"

- J. Exp. Sci.*, vol. 3, no. 1, pp. 1–4, 2012, [Online]. Available: <http://jexpsciencs.com/index.php/jexp/article/viewArticle/12469>.
- [7] C. Yiqing, “High-order Polynomial Interpolation Based on the Interpolation Center’s Neighborhood the amendment to the Runge phenomenon,” pp. 1–4, 2009, doi: 10.1109/WCSE.2009.295.
- [8] C. Ye, S. Feng, Z. Xue, C. Guo, and Y. Zhang, “Defeating Runge Problem by Coefficients and Order Determination Method with Various Approximation Polynomials,” *2018 37th Chinese Control Conf.*, pp. 8622–8627, 2018.
- [9] D. Chen, T. Qiao, H. Tan, M. Li, and Y. Zhang, “Solving the problem of Runge phenomenon by pseudoinverse cubic spline,” *Proc. - 17th IEEE Int. Conf. Comput. Sci. Eng. CSE 2014, Jointly with 13th IEEE Int. Conf. Ubiquitous Comput. Commun. IUCC 2014, 13th Int. Symp. Pervasive Syst.*, pp. 1226–1231, 2015, doi: 10.1109/CSE.2014.237.
- [10] M. Hu and F. Li, “A New Method to Solve Numeric Solution of Nonlinear Dynamic System,” *Math. Probl. Eng.*, vol. 2016, 2016, doi: 10.1155/2016/1485759.
- [11] W. P. Carey and S. S. Yee, “Calibration of nonlinear solid-state sensor arrays using multivariate regression techniques,” *Sensors Actuators B. Chem.*, vol. 9, no. 2, pp. 113–122, 1992, doi: 10.1016/0925-4005(92)80203-A.
- [12] L. Hou, T. He, and Y. Yang, “A virtual instrument for sensors nonlinear errors calibration,” *Conf. Rec. - IEEE Instrum. Meas. Technol. Conf.*, vol. 3, no. May, pp. 2103–2106, 2005.
- [13] X. jun Fan *et al.*, “A method for nonlinearity compensation of OFDR based on polynomial regression algorithm,” *Optoelectron. Lett.*, vol. 16, no. 2, pp. 108–111, 2020, doi: 10.1007/s11801-020-9047-8.
- [14] I. Balk, “Notes on Polynomial Selection for Piecewise,” *Electr. Perform. Electr. Packag. (IEEE Cat. No. 03TH8710)*, pp. 177–180, 2003.
- [15] K. Abuhmaidan, “Bijective, Non-Bijective and Semi-Bijective Translations on the Triangular Plane,” *Math. Comput. Sci.*, vol. 8, no. 1, 2020.
- [16] N. Dong and J. Roychowdhury, “Piecewise polynomial nonlinear model reduction,” *Proc. - Des. Autom. Conf.*, pp. 484–489, 2003, doi: 10.1145/775954.775957.
- [17] E. Holst and P. Thyregod, “A statistical test for the mean squared error,” *J. Stat. Comput. Simul.*, vol. 63, no. 4, pp. 321–347, 1999, doi: 10.1080/00949659908811960.
- [18] U. Khair, H. Fahmi, S. Al Hakim, and R. Rahim, “Forecasting Error Calculation with Mean Absolute Deviation and Mean Absolute Percentage Error,” *J. Phys. Conf. Ser.*, vol. 930, no. 1, 2017, doi: 10.1088/1742-6596/930/1/012002.